

A Scalable Synthesis of Adjuvanting Antigen Depots Based on Metal-Organic Frameworks

Ryanne N. Ehrman^{†a}, Olivia R. Brohlin^{†a}, Yalini H. Wijesundara^a, Sneha Kumari^a, Orikeda Trashi^a, Thomas S. Howlett^a, Ikeda Trashi^a, Fabian C. Herbert^a, Arun Raja^a, Shailendra Koirala^a, Nancy Tran^a, Noora M. Al-Kharji^a, Wendy Tang^a, Milinda C. Senarathna^a, Laurel M. Hagge^a, Ronald A. Smaldone^a, and Jeremiah J. Gassensmith^{*a,b}

^a Department of Chemistry and Biochemistry, The University of Texas at Dallas, 800 West Campbell Rd., Richardson, TX 75080, USA ^b Department of Biomedical Engineering, The University of Texas at Dallas, 800 West Campbell Rd., Richardson, TX 75080, USA.

KEYWORDS: ZIF-8 encapsulation, MOF degradation analysis, biomimetic mineralization, immune response enhancement

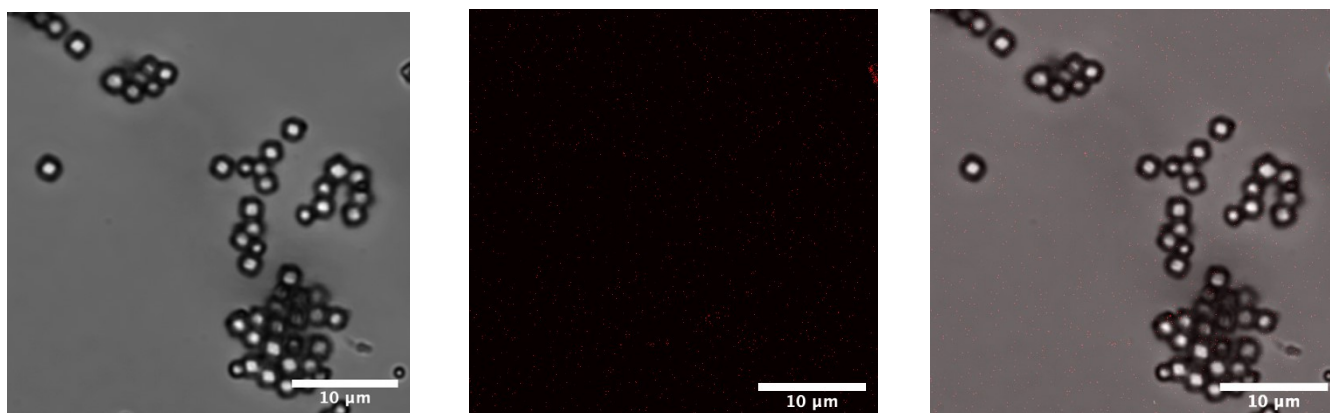


Figure S1. CLSM Images of μ -ZIF (negative control). Brightfield (left), fluorescent filter (middle), and merged channel (right) are shown. The lack of fluorescence in the fluorescent channel demonstrates that fluorescence is not from the ZIF-8.

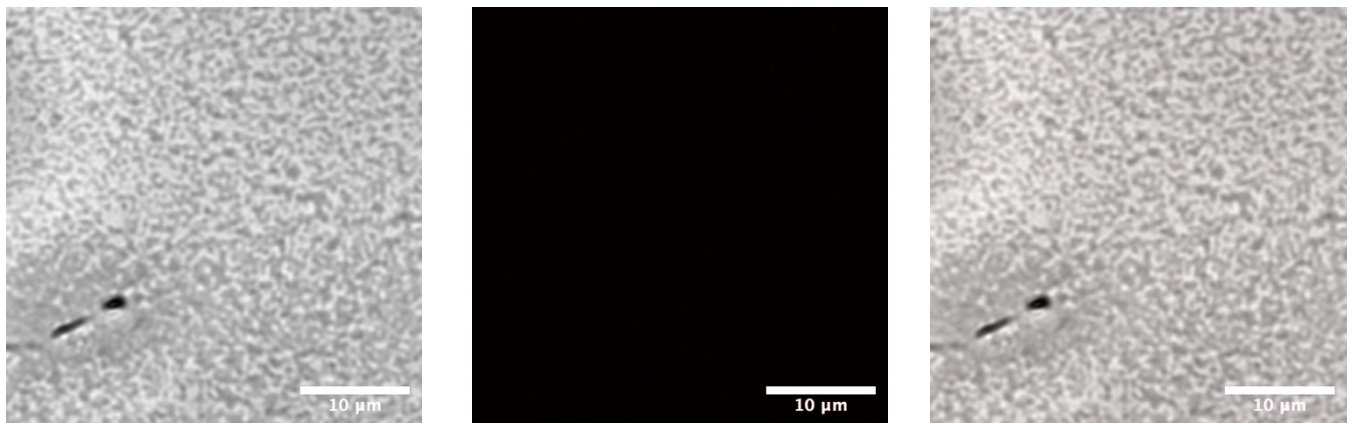


Figure S2. CLSM images of n-ZIF (negative control). Brightfield (left), fluorescent filter (middle), and merged channel (right) are shown. The lack of fluorescence in the fluorescent channel shows that fluorescence is not from the ZIF-8.

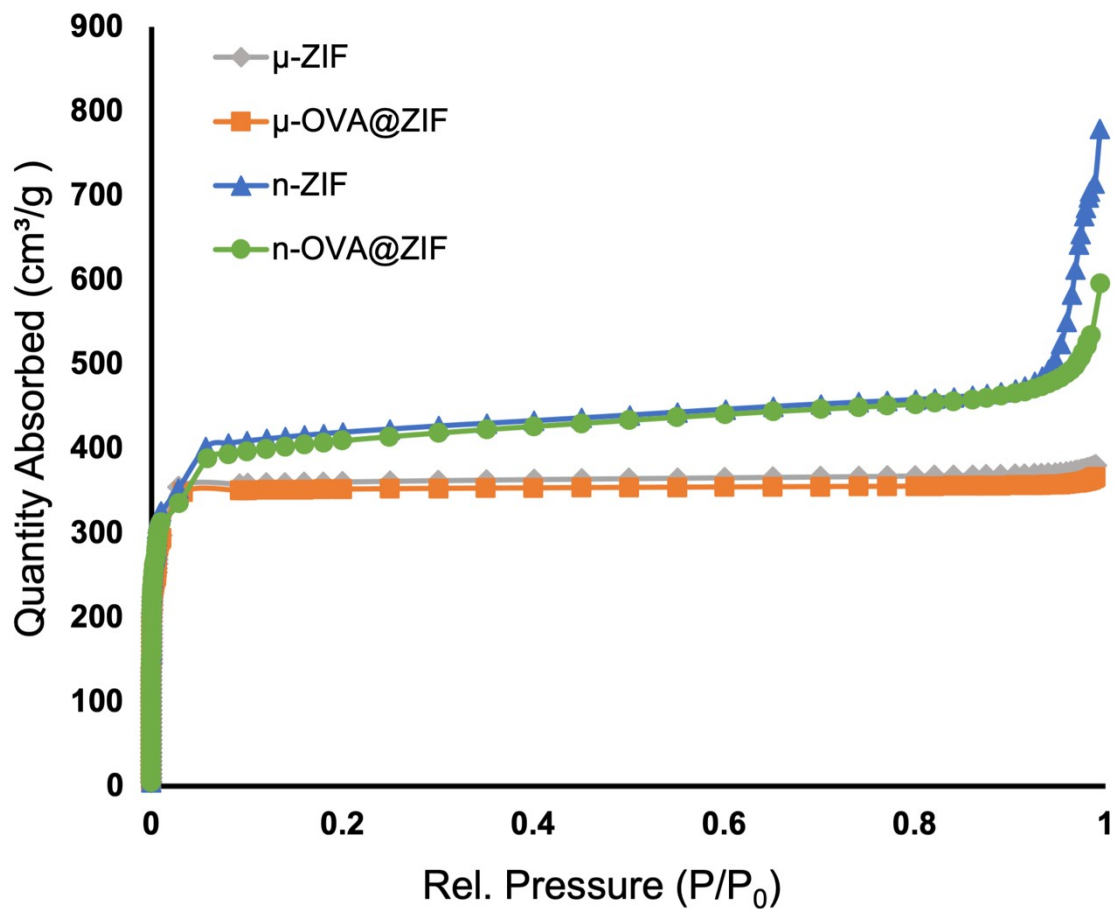


Figure S3. N₂ isotherms of ZIF and OVA@ZIF composites. Additionally, the Brunauer, Emmett, and Teller (**BET**) surface area was determined for all formulations (μ-ZIF: 1405.5495 m²/g, μ-OVA@ZIF: 1376.5082 m²/g, n-ZIF: 1645.9917 m²/g, and n-OVA@ZIF: 1601.5486 m²/g).

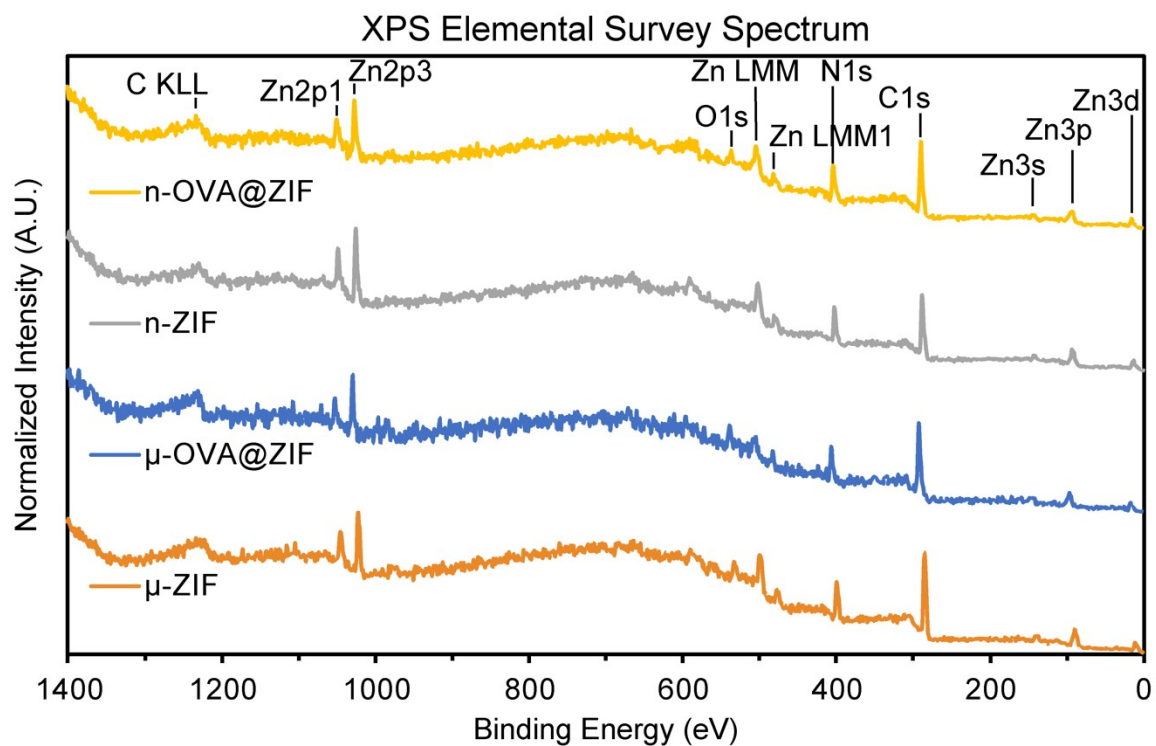


Figure S4. XPS elemental survey spectra for n-OVA@ZIF, n-ZIF, μ-OVA@ZIF, and μ-ZIF.

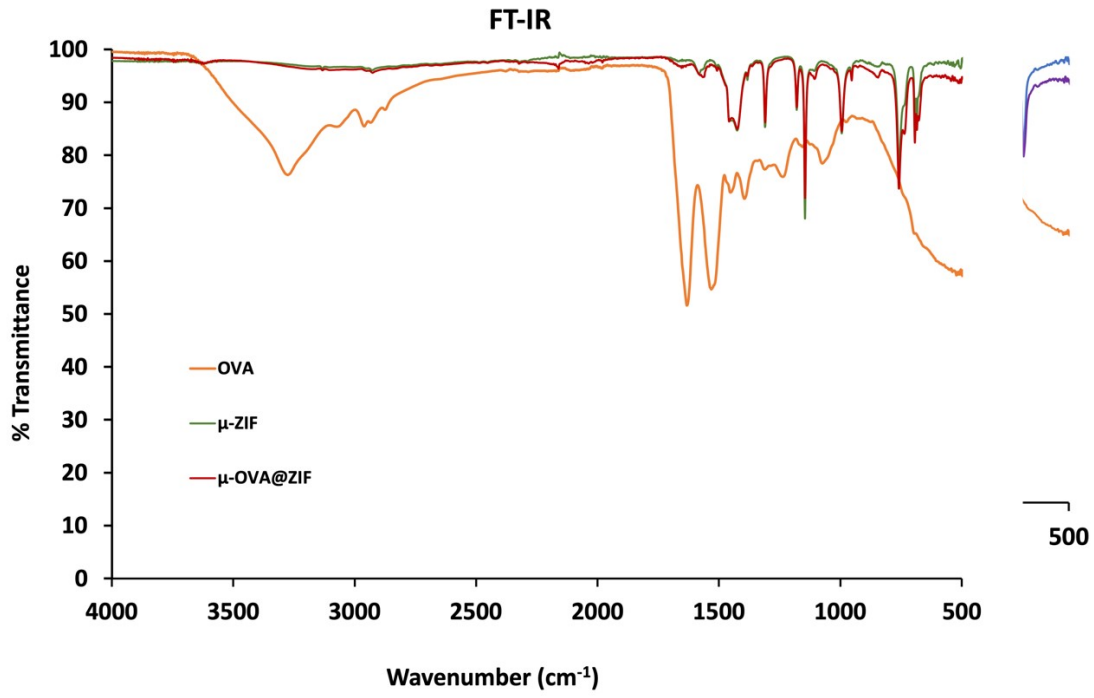


Figure S5. FT-IR spectra of n-ZIF and n-OVA@ZIF (top) and μ-ZIF and μ-OVA@ZIF (bottom).





Figure S6. Slight inflammation—raised red skin—at the injection site of n-OVA[Cy7]@ZIF post-injection.



Figure S7. Extracted ILN (left) and CILN (right) on day 14 post single-dose vaccination.

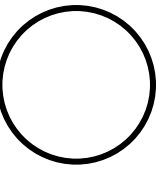


Figure S8. Post-mortem surgery to extract μ -OVA@ZIF crystals 24 h post-vaccination.

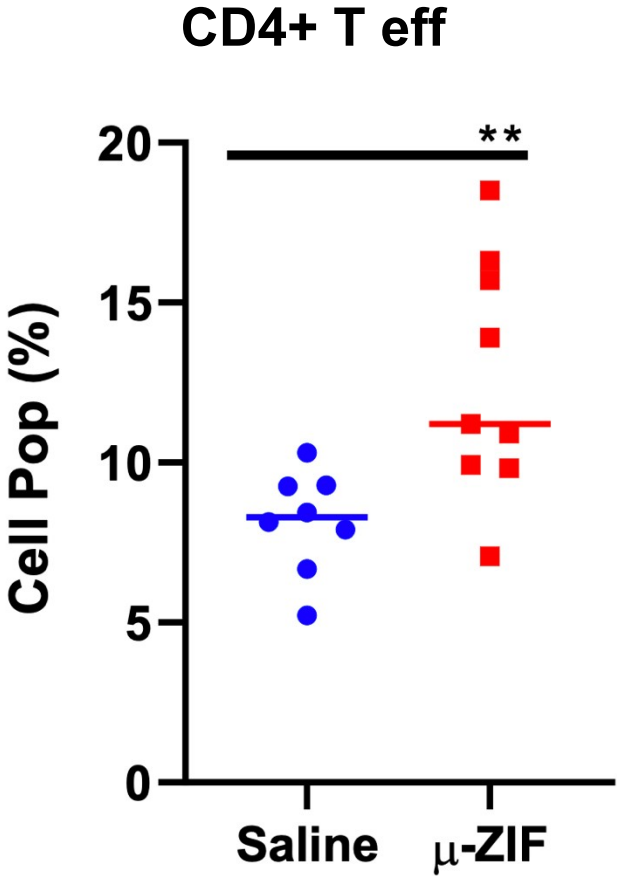


Figure S9. Percent cell populations (%) of CD4+ T eff cells (T helper cells) (CD3+/CD4+/CD44+CD62L-) in the ILN of female BALB/c mice 72 h post vaccination. Statistical significance was determined by an unpaired student's T-test ($P > 0.05$ is ns, $P \leq 0.05$ is *, $P \leq 0.01$ is **, $P \leq 0.001$ is ***, and $P \leq 0.0001$ is ****).

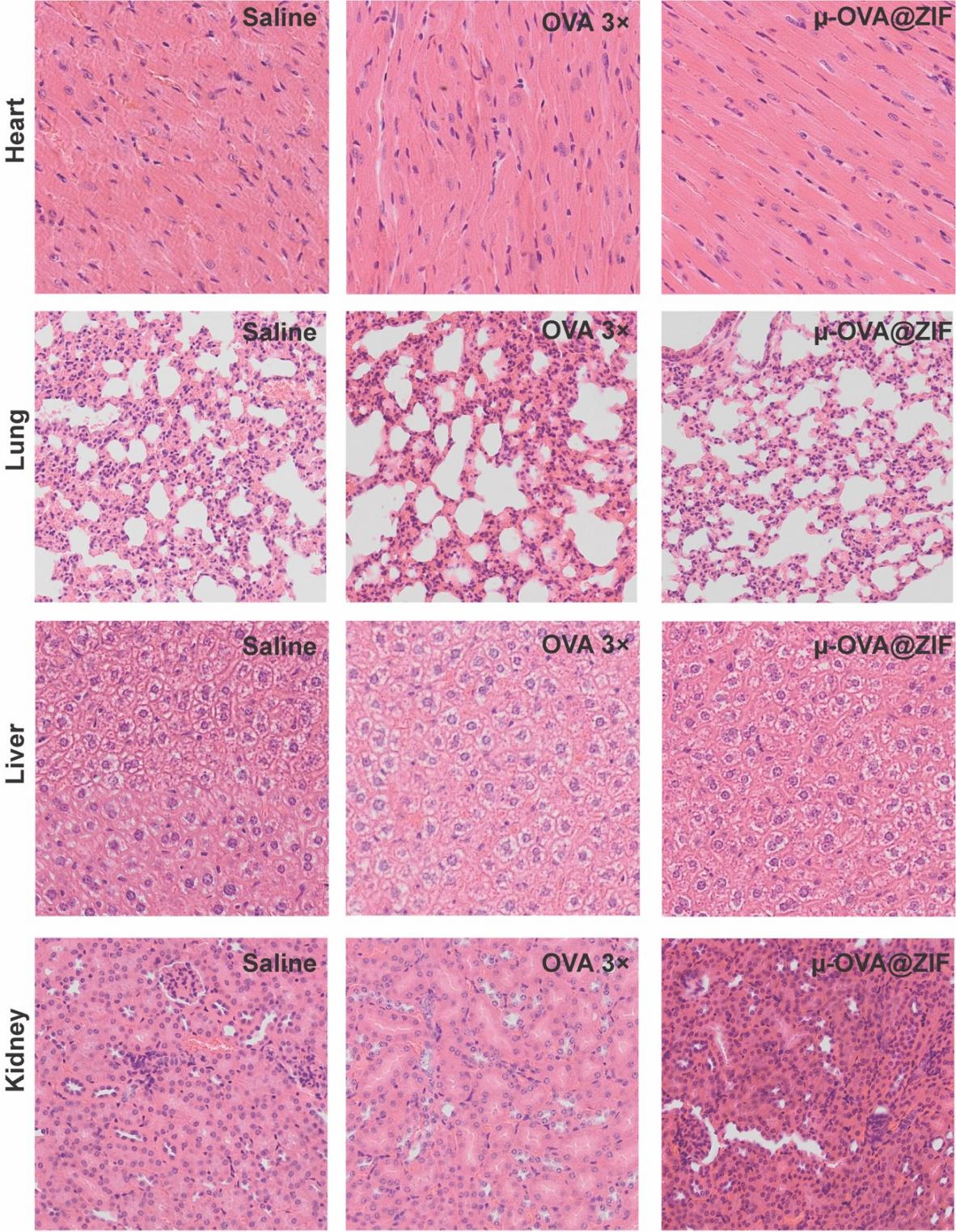


Figure S10. Day 21 H&E tissue staining of major organs.

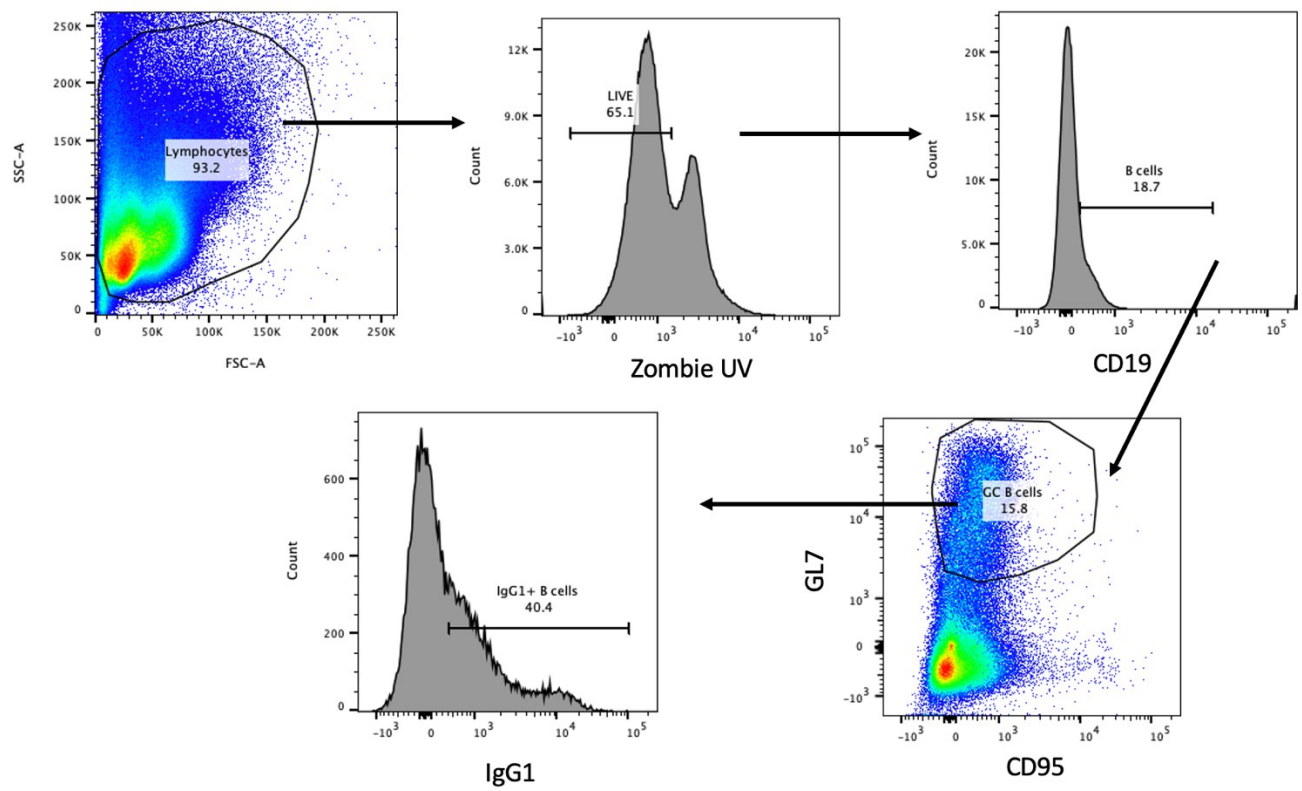


Figure S11. Gating strategy for GC B cells and IgG1+ GC B cells.

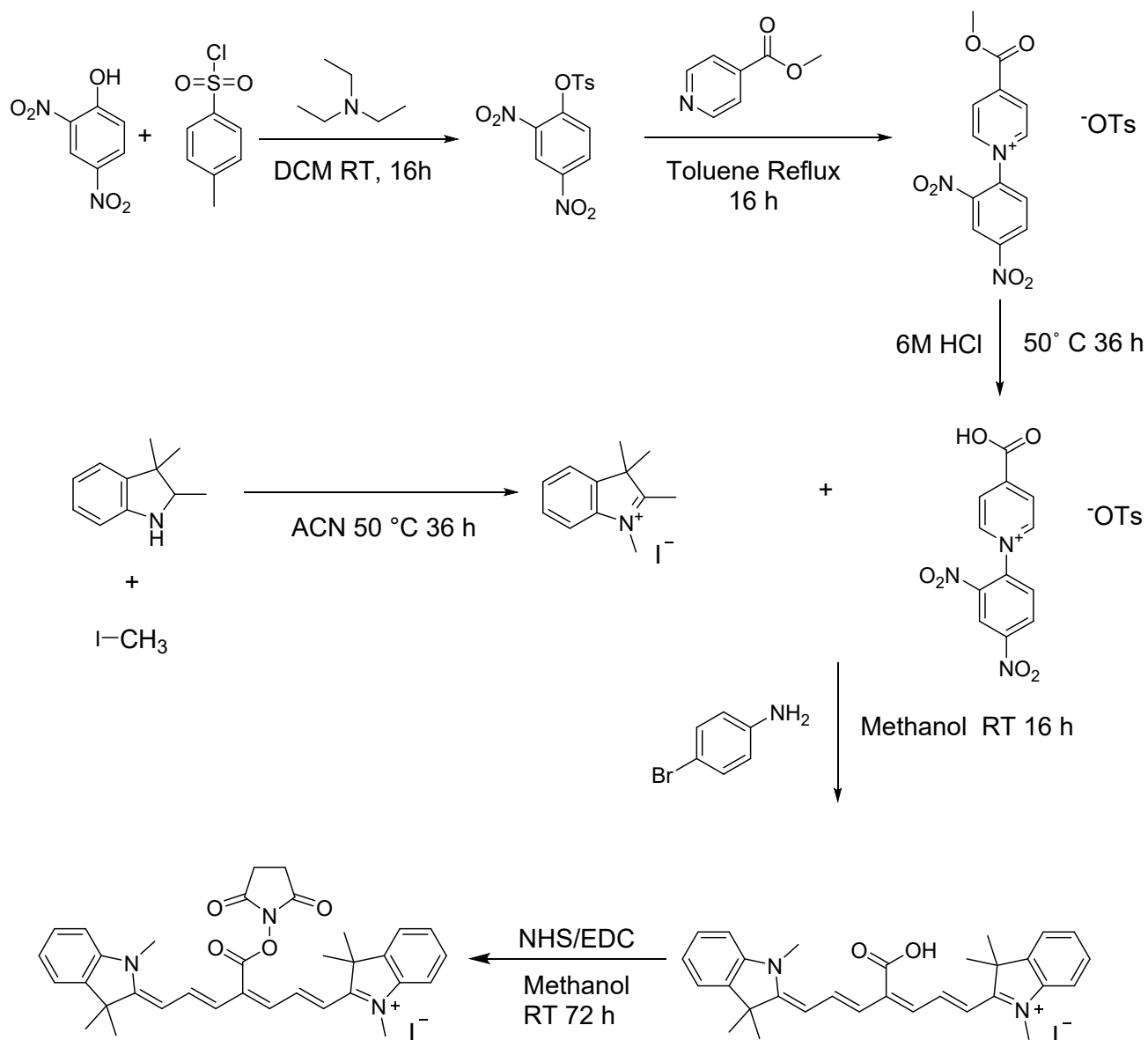


Figure S12. Synthetic Scheme for Cy7-NHS synthesis.

Cy7-NHS Synthesis

2,4-Dinitrophenyl p-Toluenesulfonate.

2,4-Dinitrophenol (2.50 g, 13.6 mmol) was dissolved in dichloromethane (50 mL), p-toluenesulfonyl chloride (2.84 g, 14.9 mmol), and triethylamine (3.45 g, 34.0 mmol) were added successively, and the mixture was stirred for 16 h at room temperature. 50 mL water was added, and the mixture was extracted with dichloromethane (3×30 mL). The organic phase was washed with NaHCO₃ (3×30 mL), brine (3×30 mL), and the organic fraction was evaporated under reduced pressure. The crude product was purified by trituration with hot methanol (30 mL) to give the pure product (white solid). Yield: 2.57 g (56%).

¹H NMR (500 MHz, d₆-DMSO): δ (ppm) 8.83 (d, J = 2.8 Hz, 1H), 8.69 – 8.47 (m, 1H), 7.91 – 7.71 (m, 2H), 7.68 – 7.35 (m, 3H), 2.46 (s, 3H).

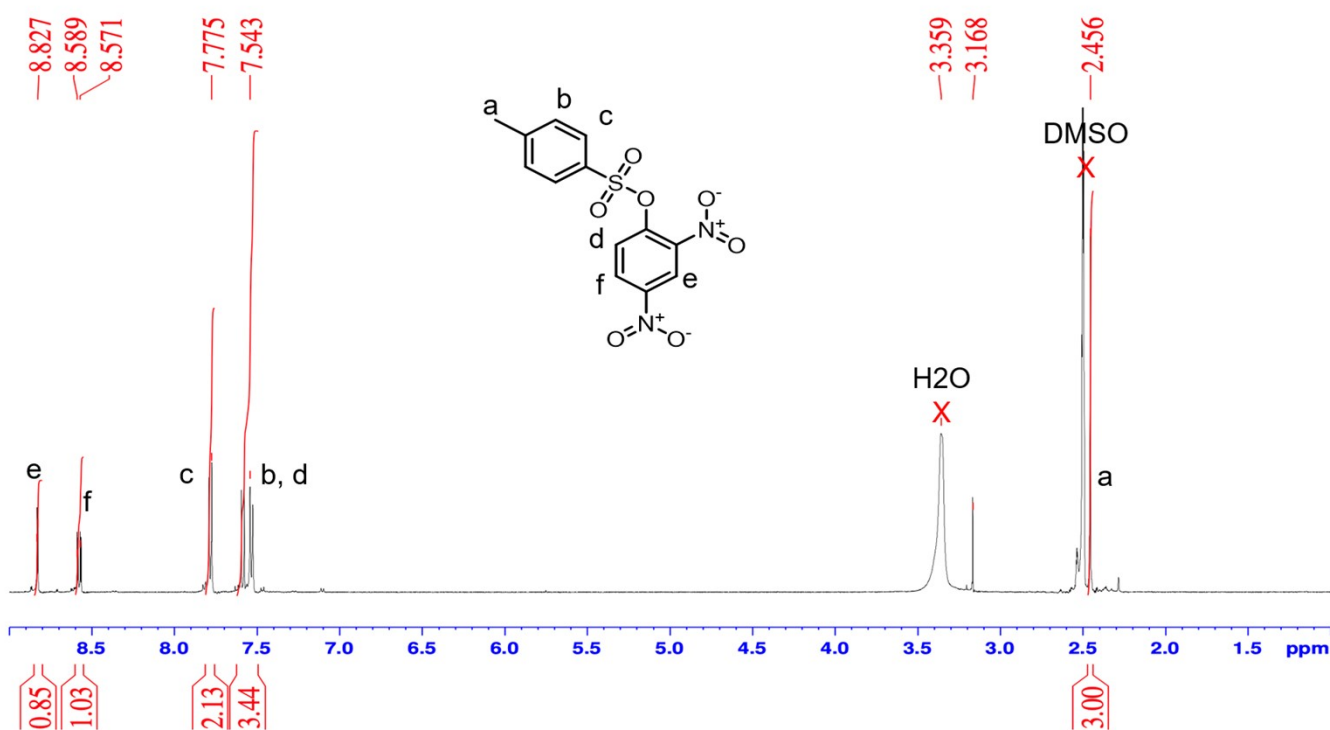


Figure S13. ¹H NMR of 2,4-Dinitrophenyl p-Toluenesulfonate

1-(2,4-Dinitrophenyl)-4-(methoxycarbonyl) pyridin-1-ium p-Toluenesulfonate

A mixture of 2,4-dinitrophenyl p-toluenesulfonate (2.57 g, 2.57 mmol) and methyl isonicotinate (0.940 g, 6.90 mmol) were dissolved in toluene (7 mL/mmol). The reaction was refluxed for 16 h and left to cool to room temperature. The precipitate was filtered, washed with toluene (2 × 5 mL) and Et₂O (2 × 5 mL), and dried. Yield: 0.78 g (24%).

¹H NMR (500 MHz, DMSO) δ 9.59 (dd, *J* = 6.7, 1.6 Hz, 2H), 9.12 (t, *J* = 1.8 Hz, 1H), 8.98 (dd, *J* = 8.7, 2.5 Hz, 1H), 8.88 – 8.75 (m, 2H), 8.40 (d, *J* = 8.7 Hz, 1H), 7.45 (dd, *J* = 8.2, 1.9 Hz, 2H), 7.10 (d, *J* = 7.8 Hz, 2H), 4.05 (s, 3H), 2.29 (s, 3H).

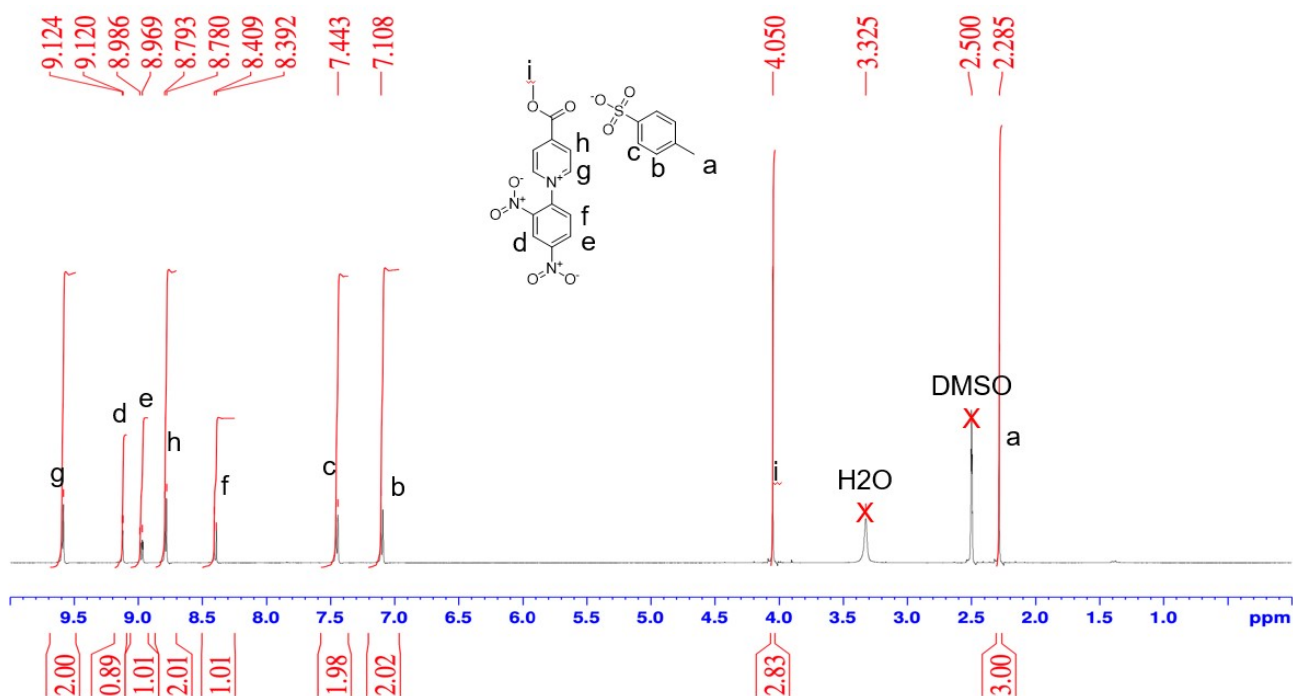


Figure S14. ¹H NMR of 1-(2,4-Dinitrophenyl)-4-(methoxycarbonyl) pyridin-1-ium p-Toluenesulfonate

4-Carboxy -1-(2,4-dinitrophenyl) pyridin-1-ium p-Toluenesulfonate

The carboxylic acid was prepared by hydrolysis of 1-(2,4-Dinitrophenyl)-4-(methoxycarbonyl) pyridin-1-ium p-Toluenesulfonate in aq HCl (6M, 50 mL) at 50 °C for 36 h. The solvent was evaporated at reduced pressure, and the crude product was purified by recrystallization from methanol (50 mL) to give the pure product as a white solid. Yield: 0.68 g (91%).

$^1\text{H NMR}$ (500 MHz, DMSO) δ 9.59 (dd, $J = 6.7, 1.6$ Hz, 2H), 9.12 (t, $J = 1.8$ Hz, 1H), 8.98 (dd, $J = 8.7, 2.5$ Hz, 1H), 8.85 – 8.70 (m, 2H), 8.40 (d, $J = 8.7$ Hz, 1H), 7.45 (dd, $J = 8.2, 1.9$ Hz, 2H), 7.10 (d, $J = 7.8$ Hz, 2H), 2.29 (s, 3H).

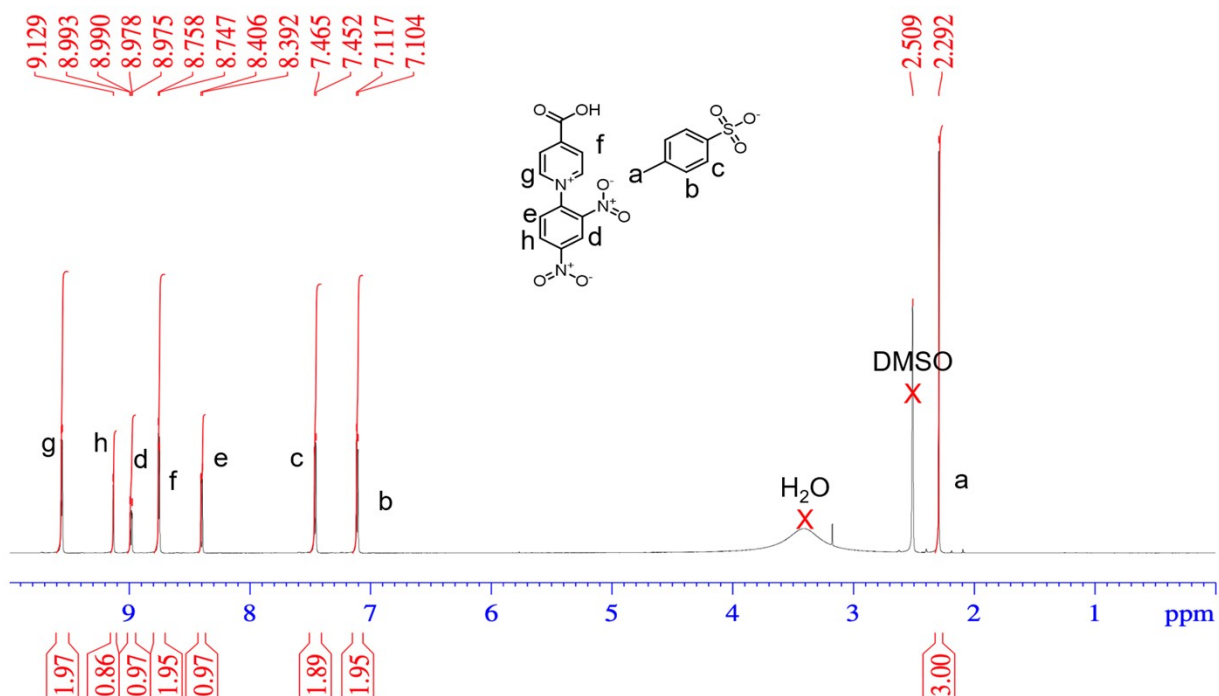


Figure S15. $^1\text{H NMR}$ of 4-Carboxy 1-(2,4-Dinitrophenyl)-4-(methoxycarbonyl)pyridin-1-ium p-Toluenesulfonate

1,2,3,3-tetramethyl-3H-indol-1-ium iodide

2,3,3-trimethylindoline (2.50 g, 15.7 mmol) and iodomethane (6.68 g, 47.1 mmol) were added to 25 ml of acetonitrile and refluxed for 5 h and cooled to RT. The white precipitate obtained was filtered and washed with acetone. The solid was dried under reduced pressure to afford 1,2,3,3-tetramethyl-3H-indol-1-ium iodide as a white solid. Yield: 2.79 g (59%). ^1H NMR (500 MHz, d_6 -DMSO) δ 7.94 – 7.86 (m, 1H), 7.86 – 7.79 (m, 1H), 7.66 – 7.57 (m, 2H), 3.97 (d, J = 1.0 Hz, 3H), 2.76 (d, J = 1.0 Hz, 3H), 1.52 (s, 6H). ^{13}C NMR (500 MHz, d_6 -DMSO): δ (ppm) 196.48, 124.58, 142.08, 129.79, 129.28, 123.76, 115.60, 54.40, 35.18, 22.18, 14.62.

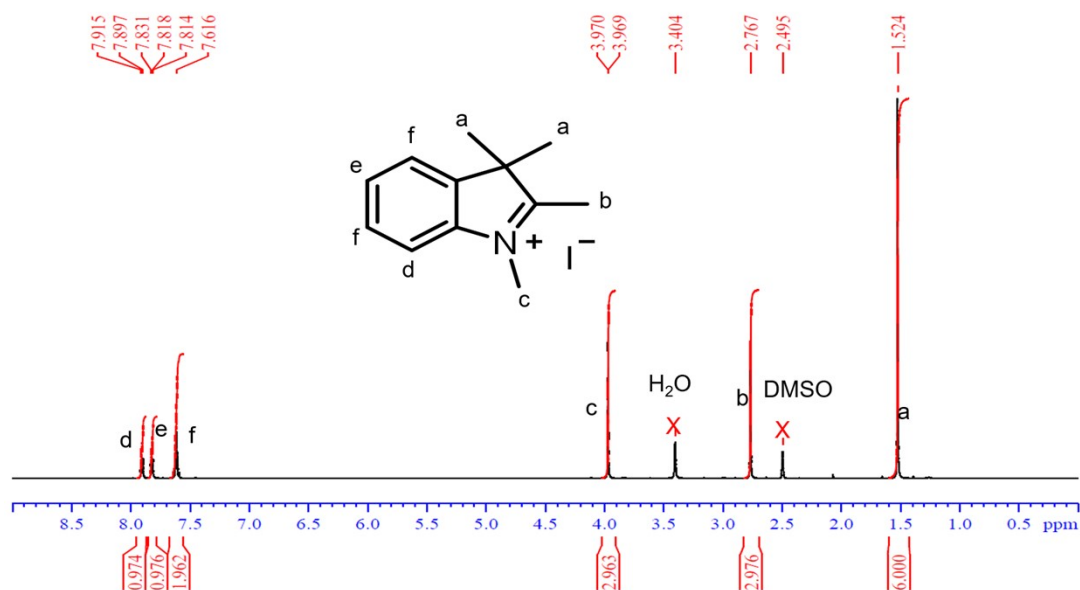


Figure S16. ^1H NMR of 1,2,3,3-tetramethyl-3H-indol-1-ium iodide.

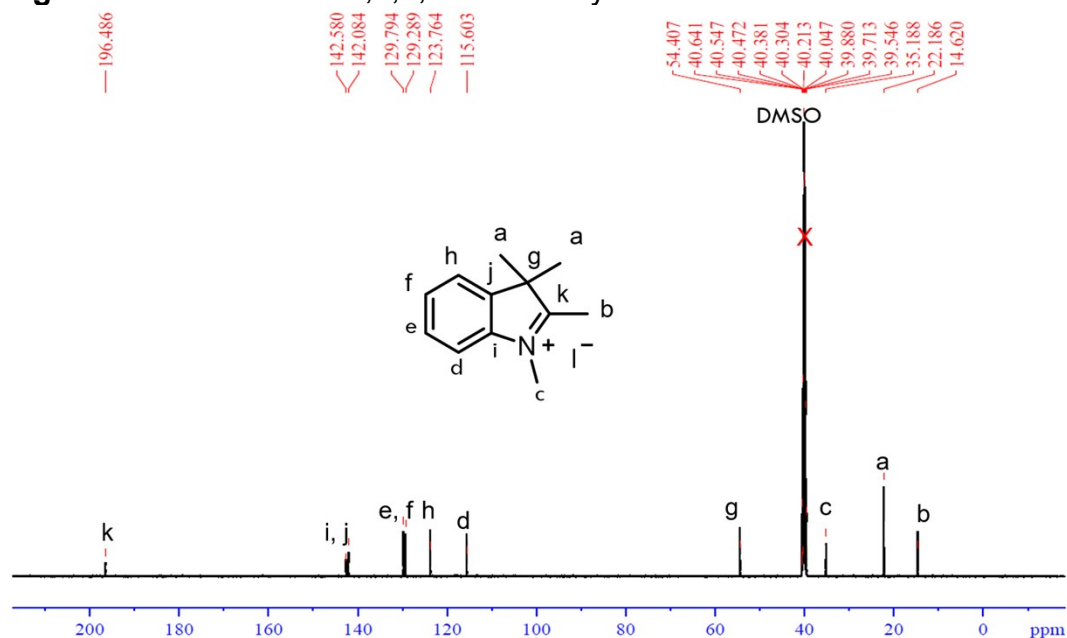


Figure S17. ^{13}C NMR of 1,2,3,3-tetramethyl-3H-indol-1-ium iodide.

2-((1E,3Z,5E)-4-carboxy-7-((Z)-1,3,3-trimethylindolin-2-ylidene) hepta-1,3,5-trien-1-yl)-1,3,3-trimethyl-3H-indol-1-ium iodide (Cy7)

4-Carboxy-1-(2,4-dinitrophenyl) pyridine-1-im p-Toluenesulfonate (161 mg, 0.540 mmol) and 4-bromoaniline (250 mg, 0.54 mmol) were dissolved in methanol (7 mL/mmol), and the mixture was stirred at RT for 30 min. Next, 1,2,3,3-tetramethyl-3H-indol-1-ium iodide (316 mg, 1.05 mmol) and sodium acetate (532 mg, 3.24 mmol) were added, and the reaction mixture was stirred for an additional 16 h at room temperature. Afterward, Et_2O (21 mL/mmol) was added, and the mixture was placed in the freezer ($-20\text{ }^\circ\text{C}$). The resulting precipitate was filtered and purified by column chromatography (silica gel, dichloromethane/methanol, 10:1, then switched to 5:1). Green solid Yield: 548 mg (69%).

^1H NMR (600 MHz, d_4 - CD_3OD): δ (ppm) 8.05 (dd, $J_1 = 13.1\text{ Hz}$, $J_2 = 13.1\text{ Hz}$, 2H), 7.39 (d, $J = 7.5\text{ Hz}$, 2H), 7.38–7.31 (m, 2H), 7.17–7.15 (m, 4H), 6.26 (dd, $J_1 = 12.6\text{ Hz}$, $J_2 = 12.6\text{ Hz}$, 2H), 6.17 (d, $J = 13.5\text{ Hz}$, 2H), 3.50 (s, 6H), 1.59 (s, 12H).

^{13}C NMR (500 MHz, d_4 - CD_3OD): δ (ppm) 173.83, 150.62, 152.9, 144.52, 142.45, 129.701, 125.92, 124.55, 123.35, 111.05, 104.59, 50.24, 31.41, 28.39.

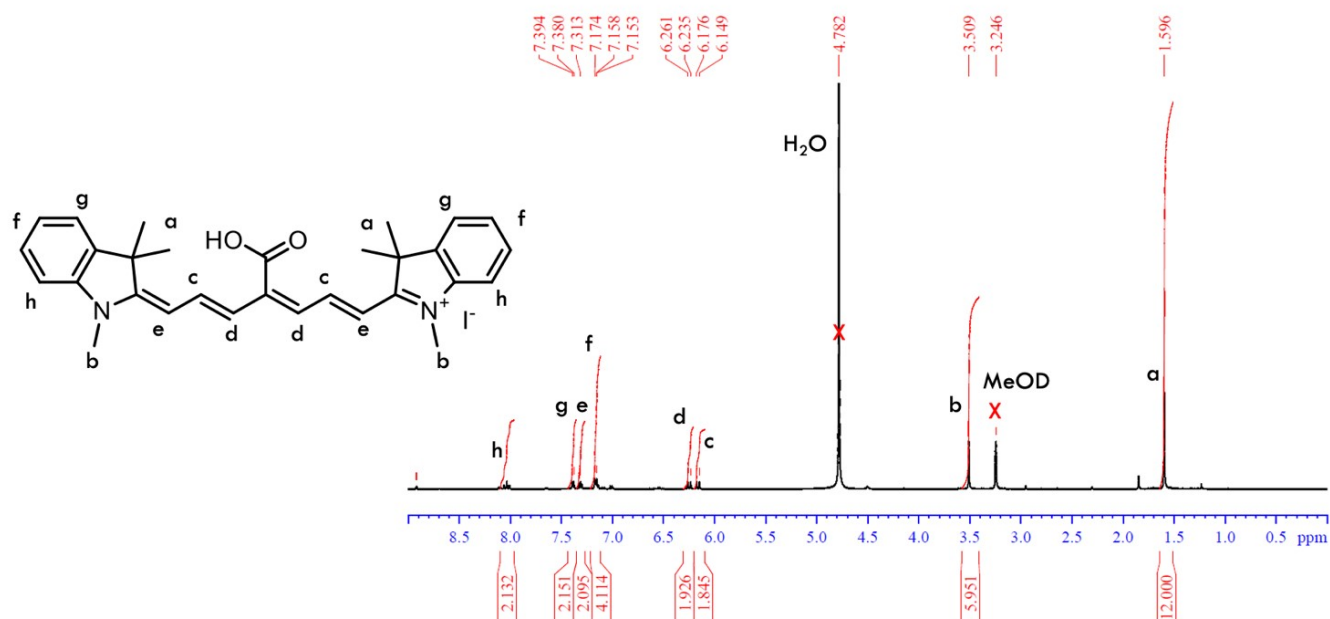


Figure S18. ^1H NMR of 2-((1E,3Z,5E)-4-carboxy-7-((Z)-1,3,3-trimethylindolin-2-ylidene) hepta-1,3,5-trien-1-yl)-1,3,3-trimethyl-3H-indol-1-ium iodide (Cy7).

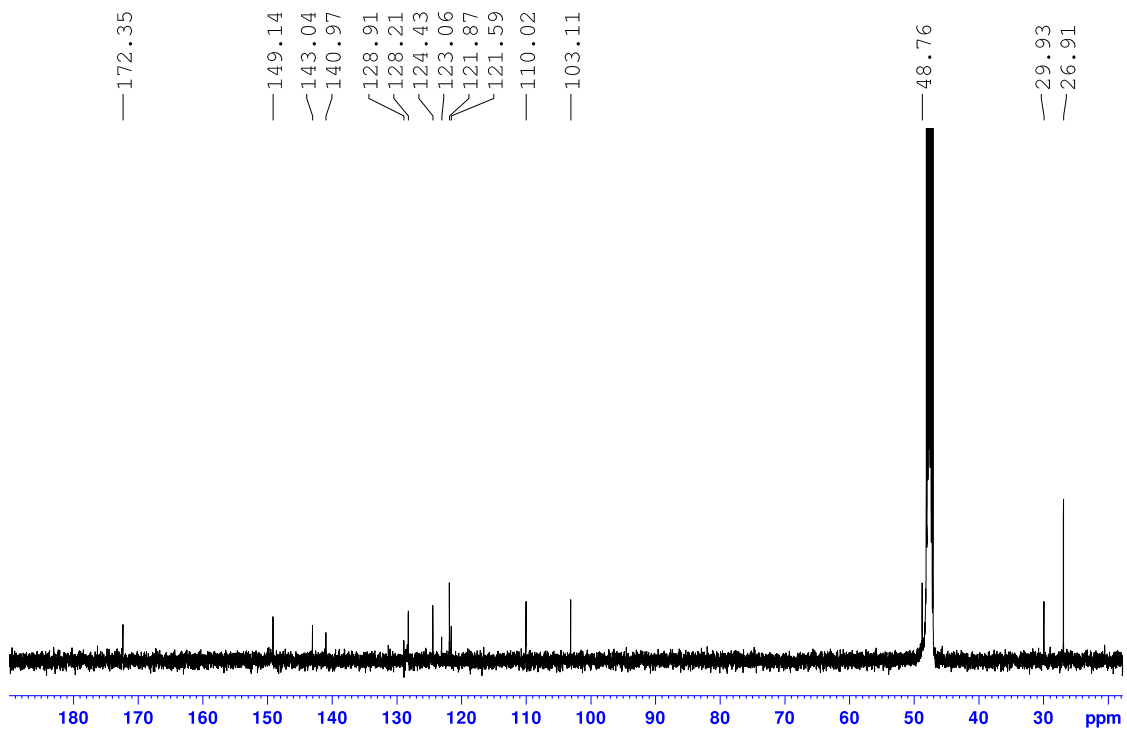


Figure S19. ¹³C NMR of 2-((1E,3Z,5E)-4-carboxy-7-((Z)-1,3,3-trimethylindolin-2-ylidene)hepta-1,3,5-trien-1-yl)-1,3,3-trimethyl-3H-indol-1-ium iodide (Cy7).

2-((1E,3Z,5E)-4-(((2,5-dioxopyrrolidin-1-yl)oxy)carbonyl)-7-((Z)-1,3,3-trimethylindolin-2-ylidene)hepta-1,3,5-trien-1-yl)-1,3,3-trimethyl-3H-indol-1-ium iodide (Cy7-NHS).

2-((1E,3Z,5E)-4-carboxy-7-((Z)-1,3,3-trimethylindolin-2-ylidene)hepta-1,3,5-trien-1-yl)-1,3,3-trimethyl-3H-indol-1-ium iodide (250 mg, 0.43 mmol), N-Hydroxysuccinimide (74 mg, 0.64 mmol) and 1-Ethyl-3-(3-dimethylaminopropyl)carbodiimide (100 mg, 0.5 mmol) were added to 10 ml of methanol and reacted for 3 days at RT. The resulting solution was purified by column chromatography. (Silica gel, dichloromethane/methanol, 10:1 then switched to 5: 1). The fraction obtained was dried under reduced pressure to afford 2-((1E,3Z,5E)-4-(((2,5-dioxopyrrolidin-1-yl)oxy)carbonyl)-7-((Z)-1,3,3-trimethylindolin-2-ylidene)hepta-1,3,5-trien-1-yl)-1,3,3-trimethyl-3H-indol-1-ium iodide as a green solid. Yield: 182 mg (63%).

^1H NMR (500 MHz, d_4 - CD_3OD) δ (ppm) 1.67 (12H, s), 3.58 (6H, s), 4.61 (4H, s), 5.50 (1H, s), 6.24 (2H, d, $J=13.57$ Hz), 6.32 (2H, d, $J=13.19$ Hz), 7.08 (1H, d, $J=9.40$ Hz), 7.23 (4H, m, $J=6.64$ Hz), 7.38 (2H, dd, $J=8.16$ Hz), 7.46 (1H, d, $J=7.33$ Hz), 8.10 (1H, t, $J=13.40$ Hz)

^{13}C NMR (500 MHz, d_4 - CD_3OD): δ (ppm) 173.36, 172.26, 149.15, 143.04, 140.97, 131.27, 128.91, 124.43, 123.07, 121.57, 110.01, 103.10, 48.78, 35.22, 29.92, 26.91.

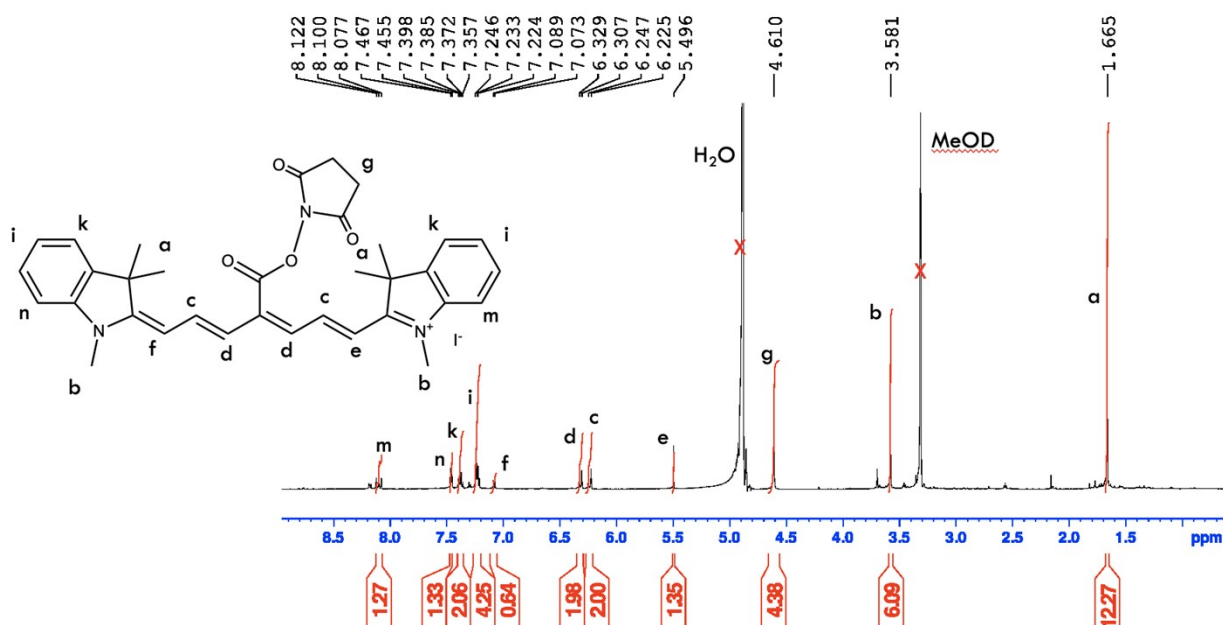


Figure S20. ^1H NMR of 2-((1E,3Z,5E)-4-(((2,5-dioxopyrrolidin-1-yl)oxy)carbonyl)-7-((Z)-1,3,3-trimethylindolin-2-ylidene)hepta-1,3,5-trien-1-yl)-1,3,3-trimethyl-3H-indol-1-ium iodide (Cy7-NHS).

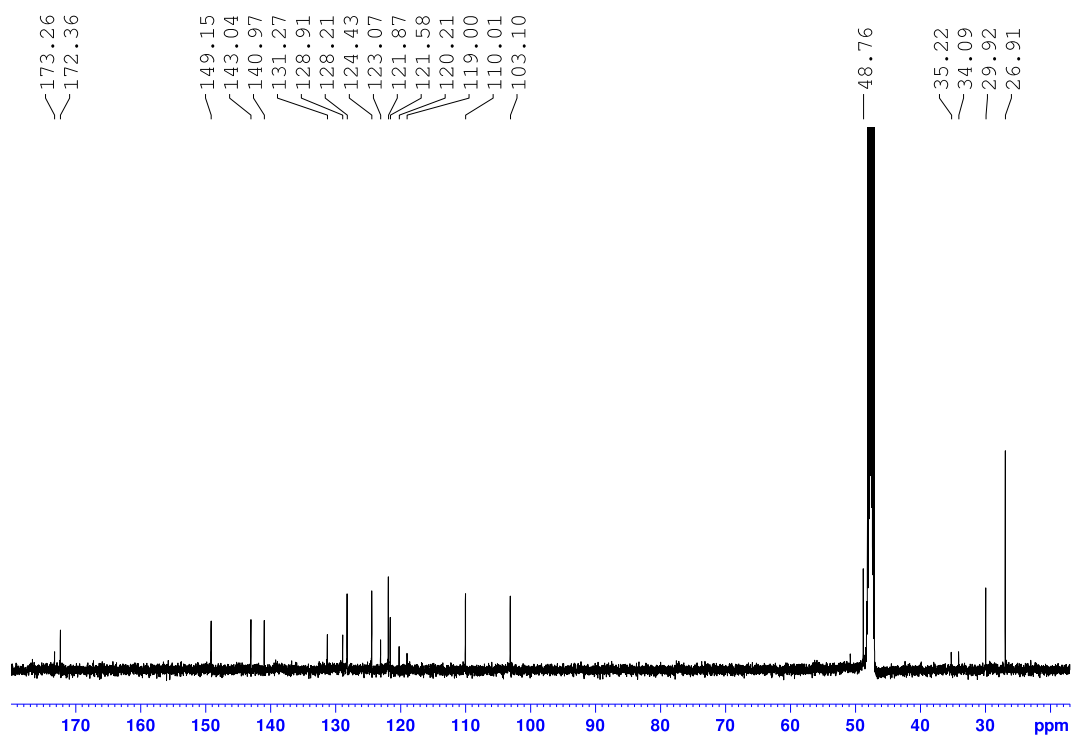


Figure S21. ^{13}C NMR of 2-((1E,3Z,5E)-4-(((2,5-dioxopyrrolidin-1-yl)oxy)carbonyl)-7-((Z)-1,3,3-trimethylindolin-2-ylidene)hepta-1,3,5-trien-1-yl)-1,3,3-trimethyl-3H-indol-1-ium iodide (Cy7-NHS)

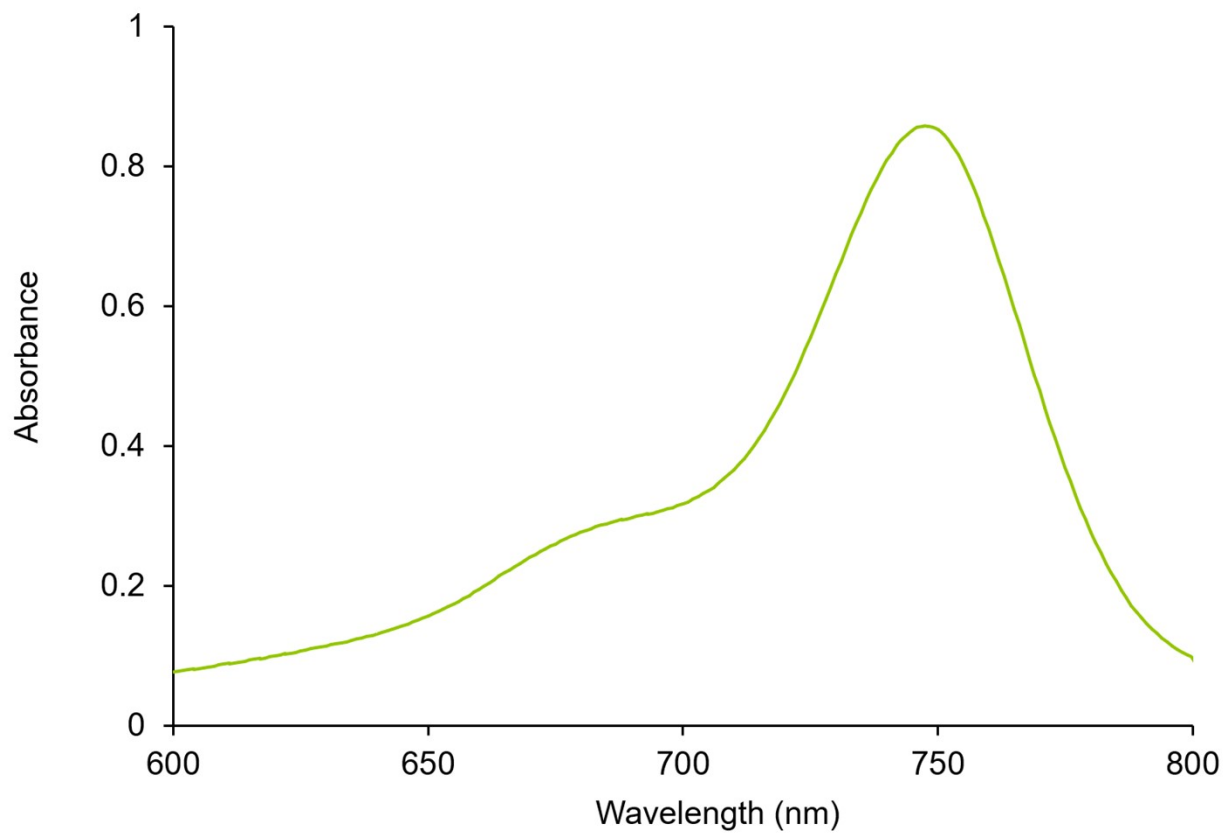


Figure S22. Absorbance spectrum of Cy7-NHS.

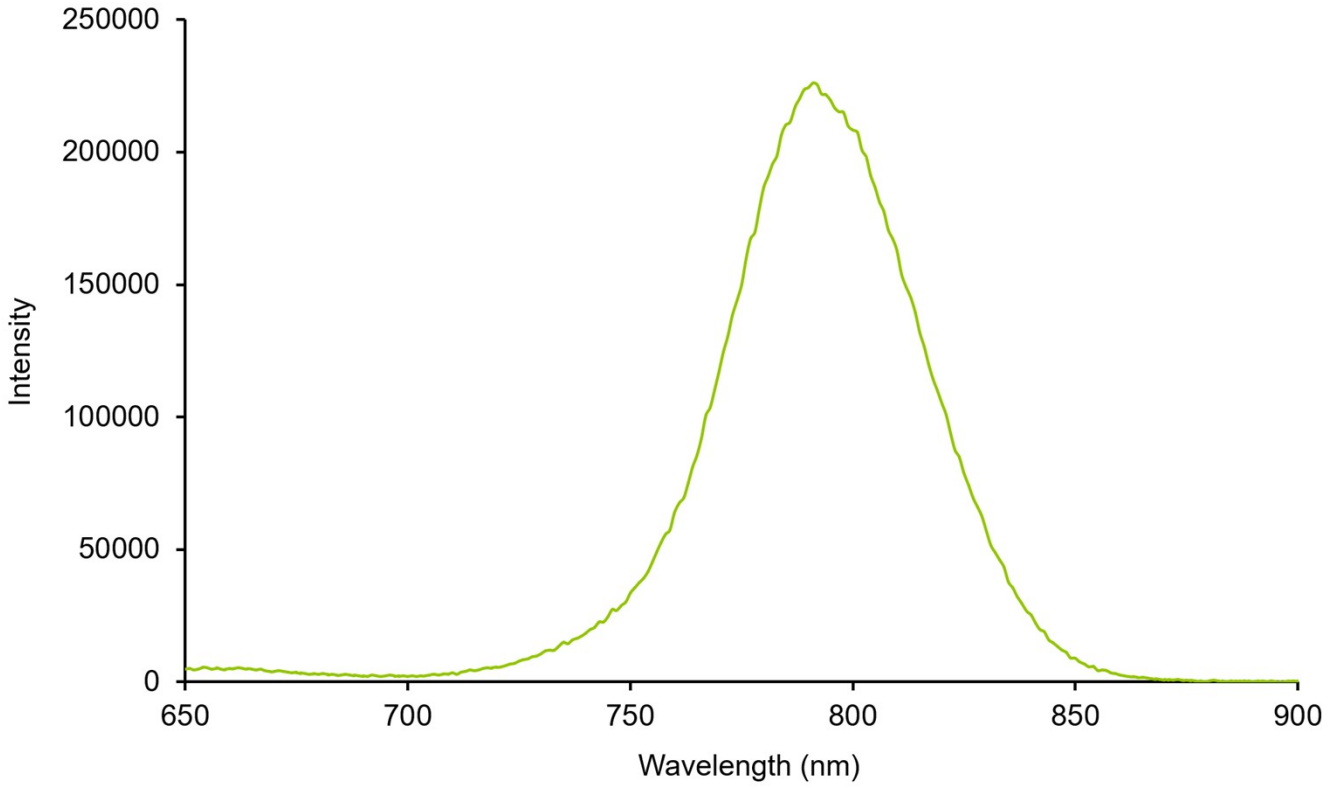


Figure 23. Emission spectrum of Cy7-NHS.